Air Gap Mixed Eccentricity Severity Detection in an Induction Motor

Rajalakshmi Samaga BL, Dr.K.P.Vittal
rajisamaga@yahoo.com , vittal_nitk@yahoo.com
Department of Electrical and Electronics Engineering, NITK- Surathkal, Karnataka, India

***Abstract*— Non invasive fault detection unit for an induction motor has become an integral part of industrial drives. As the current is the primary quantity to get affected by the non uniform air gap flux, Motor Current Signature Analysis is preferred as compared to vibration analysis for mixed eccentricity fault detection in an induction motor. In this paper, Power Spectral Density analysis is performed on the stator current data samples obtained from modeling and simulation of the induction motor. An Eccentricity Severity Factor is defined and is shown that this factor increases with increase of air gap eccentricity in the machine. Hence it can be used as a measure to assess the degree of eccentricity in the machine.**

***Index Terms*—Induction motor, Mixed eccentricity, Modeling, Power Spectral Density, Winding Function Theory**

I. INTRODUCTION

Fault diagnosis units for induction motors have become essential components in industries. It can save huge amount of money incurred by the industries due to machine failures. In this regard, model based simulation studies always help in identification of machine parameters to characterize the fault. Hence a dynamic model of induction motor operating under mixed eccentricity condition is developed using multiple coupled circuit approach. 2D-Modified Winding Function Theory (2D-MWFT) is used to calculate the mutual inductance between the windings of the machine [1-3]. The model is simulated to extract stator phase current for further analysis to characterise the fault.

Non invasive methods such as vibration analysis and motor current signature analysis (MCSA) are often employed for condition monitoring of induction motors. The author in [4], illustrates that MCSA is a powerful tool for broken rotor bar and air gap eccentricity fault detection. An added advantage of this method is that since the motor current is continuously monitored in the protection unit of the induction motor, the same unit can be employed to extract the stator current without any additional investment.

Very often mixed air gap eccentricity fault is detected by identifying the base frequency components around the fundamental frequency component in stator current spectra obtained from either Fast Fourier Transform (FFT) or Power Spectral Density analysis (PSD) [2,4-7]. It can detect the presence of mixed eccentricity condition in the machine but the severity of the fault prediction is very difficult. Hence in this paper Eccentricity Severity Factor is defined and is shown that it can be used to predict the degree of air gap eccentricity fault in the machine

The modeling methodology of an induction motor by multiple coupled circuit approach is discussed in Section II. In Section III, the simulation results obtained from the model are presented. PSD analysis results are analysed and discussed in Section IV. Conclusion is presented in Section V.

II. MODELING OF INDUCTION MOTOR FOR AIR GAP ECCENTRIC CONDITION

The machine is modeled using multiple coupled circuit approach by considering stator as 'm=3' circuits and rotor as 'n' number of rotor loops where 'n' is the total number of rotor bars. 2D-MWFT is used to calculate the mutual and self inductances between windings. The main advantage of using this method is that skewing of rotor bars can also be considered during modeling. Matlab/SIMULINK platform is used to develop the dynamic model of induction motor.

The turn functions of stator phase A and rotor loop1 are given in the Appendix. The stator turn function for the other two phases B and C are obtained by shifting the stator turn function by 60° and 120° degrees respectively. The turn functions for other rotor loops are obtained by shifting the turn function of rotor loop1 by $\alpha_r i$ where i=1,2,.n, where $\alpha_r = 2\pi/n$. The model is developed in SIMULINK platform and its block dia

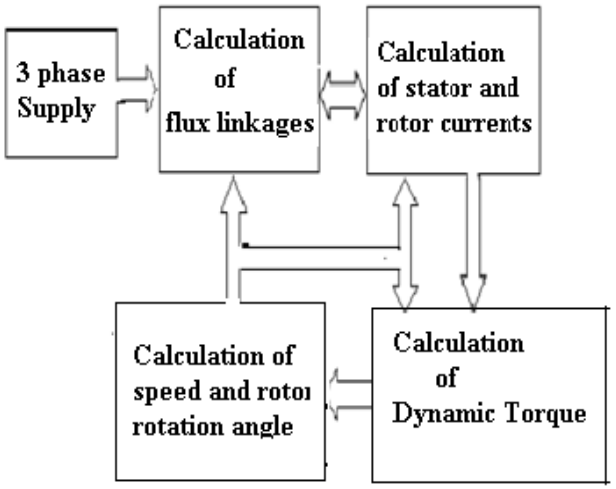

Fig1.Block diagram implementation of model

978-1-4244-9477-4/11/$26.00 ©2011 IEEE

The mutual inductance between two windings 'i' and 'j' is calculated by 2D-MWFT by using Equation (1) [1-3]. Using Equation (1), self and mutual inductances between stator phases (L_{ss}) and rotor loops (L_{rr}) and mutual inductance between stator and rotor loops (L_{sr}) are calculated.

$$L_{ij}(\theta_r) = \sum_{z=1}^{z=11} L_{ij}(\theta_r, z) \qquad -(1)$$

where $L_{ij}(\theta_r, z) = 2\pi\mu_0 r\left[\langle Pn_i n_j\rangle - \frac{\langle Pn_i\rangle\langle Pn_j\rangle}{\langle P\rangle}\right] * \frac{l}{11}$

where

L_{ij}=mutual inductance between the windings 'i' and 'j' in H
θ_r = rotor rotation angle in radians
z=section along axial length of rotor
n_i=turn function of winding 'i'
n_j=turn function of winding 'j
μ_0=absolute permeability
r=radius in m
l =length of stack in m
P= permeance of air gap in m^{-1}

Equation (2) is used to calculate the permeance of the air gap which can take into account mixed eccentricity condition prevailing in the machine.

$$P(\emptyset, z, \theta_r) = p_0(z) + p_1(z)\cos(\emptyset - \rho(z)) + p_2(z)\cos(2\emptyset - 2\rho(z)) \qquad -(2)$$

where p_0, p_1, p_2 and ρ are calculated as

$$\rho(z) = \tan^{-1}\left(\frac{\delta_d(z)\sin(\theta_r)}{\delta_s(z) + \delta_d(z)\cos(\theta_r)}\right)$$

$$\delta(z) = \sqrt{\delta_s^2(z) + \delta_d^2(z) + 2\delta_s(z)\delta_s(z)\cos(\theta_r)}$$

$$p_0(z) = \frac{1}{g_0}$$

$$p_1(z) = 2\left(\frac{1}{g_0\sqrt{1-\delta^2(z)}}\right)\left(\frac{1-\sqrt{1-\delta^2(z)}}{\delta(z)}\right)$$

$$p_1(z) = 2\left(\frac{1}{g_0\sqrt{1-\delta^2(z)}}\right)\left(\frac{1-\sqrt{1-\delta^2(z)}}{\delta(z)}\right)^2$$

where δ_s and δ_d represent the static and dynamic eccentricity indices respectively.

The resistances and inductances for each rotor rotation angle are calculated in 'm' files and brought to the SIMULINK model during simulation. Simulation results are discussed in the following section.

III. SIMULATION RESULTS

The machine parameters considered for modeling and simulation are given in the Appendix. The model is simulated using Runge-Kutta4 and fixed step size of 0.00005seconds for the eccentric condition of 40% static eccentricity and 30% dynamic eccentricity in the machine. The simulated waveforms are as shown in Figure2. The nominal load of 12 Nm is applied at 1second. The developed machine model can take the load even at the starting of simulation.

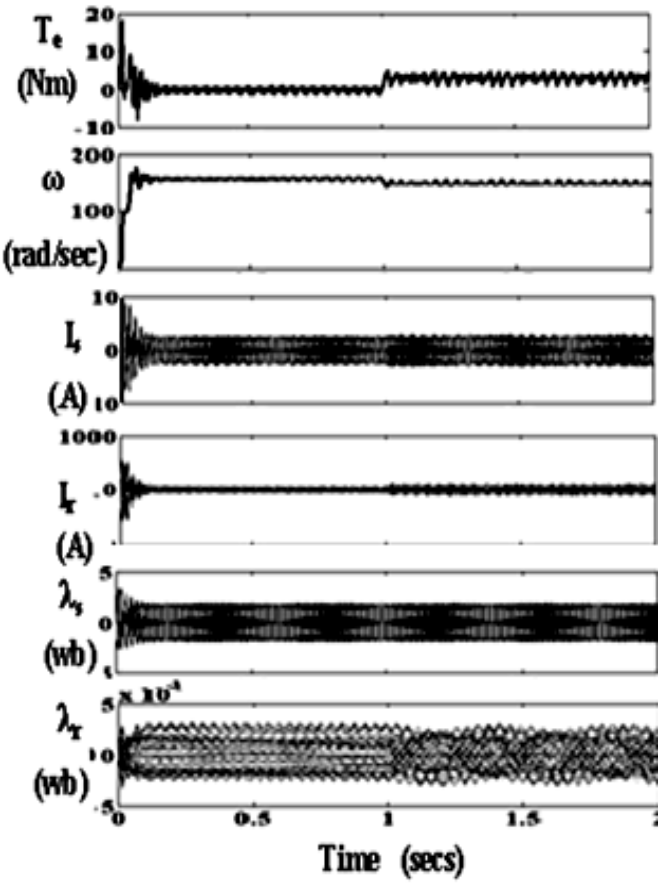

Fig2. Dynamic Torque (T_e) vs. Time, Speed (ω) vs. Time, Stator phase currents (I_s) vs. Time, Rotor loop currents (I_r) vs. Time, Stator flux linkages (λ_s) vs Time, Rotor flux linkages (λ_r) vs. Time

During simulation, 20000 samples of stator phase current of the machine at sampling frequency of 20 kHz are extracted and stored for offline studies. All these data are filtered after passing through a10kHz low pass filter using Hann window. Further, analysis is carried out on these data to detect the eccentricity fault which are explained in the following chapter.

IV. PSD ANALYSIS

Usually, Fast Fourier Transform (FFT) and Power Spectral Density (PSD) analysis are performed on the stator current to detect the presence of eccentricity in the machine. The results obtained by the PSD analysis carried out on the extracted stator current data of the machine with 40% static eccentricity and 30% dynamic eccentricity prevailing in the machine is as shown in Figure3.

The existence of sideband frequencies (f_1 and f_2) around the base frequency, at **73.57 Hz and 26.43 Hz** under loaded conditions are mainly due to prevailing mixed eccentricity condition in the machine. If both static (SE) and dynamic eccentricities (DE) exist together, low frequency components near the fundamental [10] given by

$$f_e = \left(1 \pm \frac{k}{p}(1-s)\right).f \qquad k = 2,3 \ldots\ldots \qquad -(3)$$

can be detected for all machines.

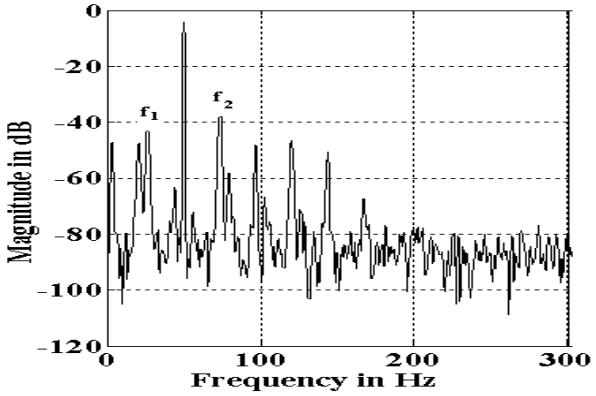

Fig3. PSD analysis with 40% SE and 30% DE

PSD analysis results are verified with theoretically calculated values of **75.68 Hz and 24.41 Hz** for no load, and **73.24 Hz and 26.86 Hz** for loaded conditions using the Equation (3) where 'p' is the number of pole pairs, 's' is the slip and 'f' is the fundamental frequency.

The presence of static and dynamic eccentricity can be detected using MCSA [10]. The equation describing the frequency components of interest is

$$f_e = f_1\left[(kR \pm n_d)\frac{(1-s)}{p} \pm v\right] \quad -(4)$$

Where n_d=0 in case of static eccentricity and n_d=1,2,3…….in case of dynamic eccentricity (n_d is known as eccentric order), f_1 is the fundamental frequency, R is the number of rotor slots, s is the slip, p is the number of pole pairs, k is any integer, and v is the stator harmonics that are present in the power supply driving the motor (v=±1,±3,±5).

If both static and dynamic eccentricities exist together, low-frequency components near the fundamental given by the Equation (3) can be detected for all machines. These low-frequency components also give rise to high-frequency components as described by Equation (4)

However, these components are strong only for machines whose pole pairs and rotor slot numbers are related by

$$R = 2p[3(m \pm q) \pm r] \pm k \quad -(5)$$

where , m±q=0,1,2,3,4…. and r=0 or 1, k=1 or 2 .

It has been reported in the literature that with k=2, these components are very weak and noticeable only under light load conditions. [9]

For the machine chosen R=30, p=2

$$2p[3(m \pm q) \pm r] \pm k = 2 * 2[3 * 3 - 1] - 2 = 30$$
$$2p[3(m \pm q) \pm r] \pm k = 2 * 2[3 * 2 + 1] + 2 = 30$$

Since the Equation (2) is valid only for k=2, the high frequency components will be very weak and noticeable only under light load conditions. For the machine chosen, these high frequency components were found to be weak from PSD analysis. Hence was not considered for further analysis.

PSD analysis gives information about the existence of eccentricity but interpreting the degree of eccentricity is very difficult as the margin of variation between these frequencies is negligible. Authors [11] in their paper illustrate that DE increases the amplitude of sideband components around PSH which can be used for detection of dynamic eccentricity and when the SE is increased, the amplitude of the sideband components is increased as well; however, for a fixed load, the frequency of sideband components due to the fault remain constant..In the same paper it is reported that noise can affect this index and fault diagnosis may produce an error.

Table 1-3, gives the details about sideband frequencies around the base frequency for the machine which has developed 20% dynamic eccentricity and variable static eccentricities for full load (14.89 Nm), 53% load (8Nm) and no load conditions respectively. Frequency resolution considered is 1 Hz for PSD analysis.

Table1: Full load with 20% dynamic eccentricity

%SE	f_1 and magnitude		Base frequency		f_2 and magnitude	
10	26	-52.79	50	-3.9	74	-44.94
20	26	-47.8	50	-4	74	-43.81
30	26	-45.34	50	-4.07	74	-40.31
40	26	-43.07	50	-4.13	74	-38.03
50	26	-36.42	50	-4.15	74	-36.98

Table2: 53% load with 20% dynamic eccentricity.

%SE	f_1 and magnitude		Base frequency		f_2 and magnitude	
10	26	-50.99	50	-4.35	74	-43.55
20	26	-43.78	50	-4.46	74	-43.92
30	26	-40.91	50	-4.53	74	-40.37
40	26	-38.82	50	-4.61	74	-38.09
50	26	-34.76	50	-4.65	74	-37.22

Table3: No load with 20% dynamic eccentricity.

%SE	f_1 and magnitude		Base frequency		f_2 and magnitude	
10	25	-46.25	50	-4.51	74	-44.82
20	25	-39.45	50	-4.63	74	-47.89
30	25	-35.79	50	-4.71	74	-44.78
40	25	-36.36	50	-4.79	74	-40.15
50	25	-32.5	50	-4.88	74	-46.09

From Table1-3, following observations are made

1. Amplitude of fundamental frequency in dB decreases with increase in static eccentricity.
2. Amplitude of side band frequencies in dB increases with increase in static eccentricity.(except no load)
3. The side band frequency components around fundamental remain the same with increase in static eccentricity.
4. Observation 3 can be attributed to the facts that speed and hence slip is not affected with the increase in static eccentricity.

Table 4-6, gives the details about sideband frequencies around the base frequency for the machine which has

developed 40% static eccentricity and variable dynamic eccentricities for full load (14.89 Nm), 53% load (8Nm) and no load conditions respectively.

Table4: Full load with 40% static eccentricity.

%DE	f_1 and magnitude		Base frequency		f_2 and magnitude	
3	27	-59.59	50	-4.01	73	-55.08
5	27	-55.48	50	-4.01	73	-50.52
7	27	-52.58	50	-4.02	73	-47.61
10	26	-49.48	50	-4.04	74	-44.53
20	26	-43.07	50	-4.13	74	-38.03
30	26	-38.62	50	-4.28	74	-33.94
40	26	-33.32	50	-4.46	74	-29.83

Table5: 53% load with 40% static eccentricity

%DE	f_1 and magnitude		Base frequency		f_2 and magnitude	
3	26	-55.38	50	-4.64	74	-54.82
5	26	-50.96	50	-4.47	74	-50.39
7	26	-48.09	50	-4.49	74	-47.43
10	26	-44.92	50	-4.49	74	-44.53
20	26	-38.82	50	-4.61	74	-38.03
30	26	-35.28	50	-4.79	74	-33.66
40	26	-32.38	50	-5.03	74	-29.18

Table6: No load with 40% static eccentricity

%DE	f_1 and magnitude		Base frequency		f_2 and magnitude	
3	25	-52.14	50	-4.63	75	-58.81
5	25	-47.49	50	-4.63	75	-54.48
9	25	-44.56	50	-4.64	75	-51.24
10	25	-41.78	50	-4.66	75	-47.48
20	25	-36.36	50	-4.79	75	-40.15
30	25	-36.82	50	-4.99	75	-33.65
40	25	-34.44	50	-5.23	75	-31.64

From Table4-6, following observations are made

1. Amplitude of fundamental frequency in dB decreases with the increase in dynamic eccentricity.
2. Amplitude of side band frequencies in dB increases with increase in static eccentricity.
3. The side band frequency components around fundamental change with increase in dynamic eccentricity.(refer Table 4)
4. Observation 3 can be attributed to the fact that with the increase in dynamic eccentricity, speed with which machine runs increases and slip decreases.

In this paper Eccentricity Severity Factor (ESF) is defined as

$$ESF1 = \frac{(\text{Amplitude of base frequency in dB} - \text{Amplitude of lower side band frequency in dB})}{\text{Amplitude of base frequency in dB}}$$

and

$$ESF2 = \frac{(\text{Amplitude of base frequency in dB} - \text{Amplitude of upper side band frequency in dB})}{\text{Amplitude of base frequency in dB}}$$

Total Indicated Reading (TIR) of the motor provided by the manufacturer controls the dynamic eccentricity level in the machine. Even though 10% eccentricity is permissible, manufacturer keeps this value as low as possible. Static eccentricity exists in the machine even at the assembly stage. For a stiff rotor shaft assembly like the chosen machine for analysis, static eccentricity is unlikely to change. Hence ESF are calculated for fixed static eccentricity value, with dynamic eccentricity values being varied.

Eccentricity severity factors are calculated from the extracted stator currents obtained via simulation of the machine model for the machine running condition of 40% static eccentricity and varied dynamic eccentricities. Calculated ESF1 and ESF2 values for the machine under full load, half load and no load are presented inTable7.

Table7: %DE and ESF1 and ESF2 values.

	Full load		53% load		No load	
%DE	ESF1	ESF2	ESF1	ESF2	ESF1	ESF2
3	-13.86	-12.74	-10.94	-10.81	-10.26	-11.70
5	-12.84	-11.60	-10.40	-10.27	-9.26	-10.77
7	-12.08	-10.84	-9.71	-9.56	-8.60	-10.04
10	-11.25	-10.02	-9.00	-8.92	-7.97	-9.19
20	-9.43	-8.21	-7.42	-7.25	-6.59	-7.38
30	-8.02	-6.93	-6.37	-6.03	-6.38	-5.74
40	-6.47	-5.69	-5.4	-4.80	-5.59	-5.05

Using Table7, variation of ESF1 and ESF2 are plotted against %DE and are shown in Figures4-5 for full load, half load and no load conditions of the machine

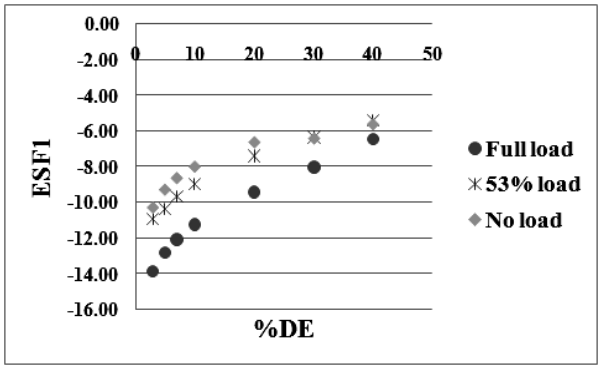

Fig4. %DE vs. ESF1

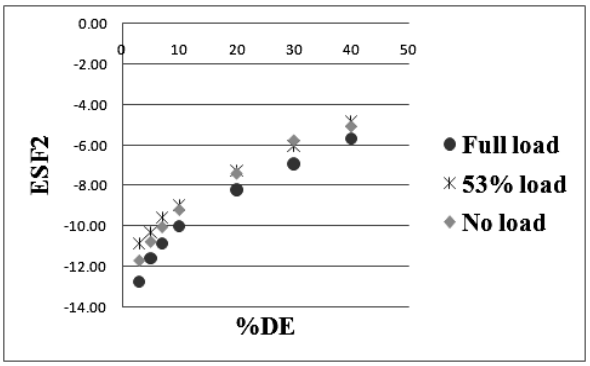

Fig5. %DE vs. ESF2

From Figures 4-5, it is concluded that eccentricity fault severity factor increases with the increase in dynamic eccentricity for an existing 40% static eccentricity in the machine.

V. CONCLUSION

In this paper, an induction motor is modeled using 2D-MWFT and simulated for different eccentricity conditions. Samples of stator current are extracted and stored for offline studies.PSD analysis is performed on these data showed that presence and degree of mixed air gap eccentricity can be predicted very effectively. An Eccentricity Severity Factor is defined and is shown that it increases with the increase in air gap eccentricity. Hence it can be used to predict the degree of a mixed air gap eccentricity prevailing in the machine.

APPENDIX

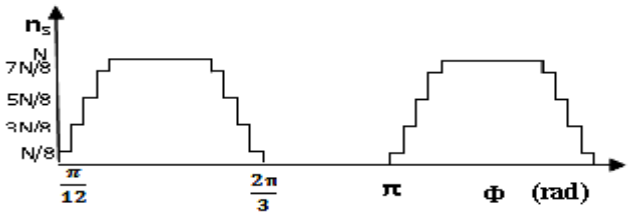

Stator Phase A turn function

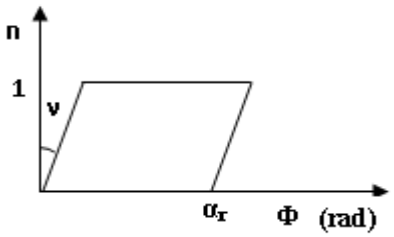

Rotor loop 1 turn function

2.2kW, 3hp,400/415V, 50Hz, 3ΦAC,1500rpm, 4pole squirrel cage induction motor
Number of stator slots =24, Number of rotor bars =30,
Length of stacks =120mm, Effective air gap =0.35mm,
Mean radius of air gap=89.65mm,
Number of turns/phase =400, Stator resistance =7.6Ω,
Stator leakage inductance =38.43mH,
Rotor bar resistance=0.00376Ω,
Rotor bar leakage inductance =44.52μH,
Rotor end ring segment resistance =0.0012 mΩ,
Rotor end ring segment inductance =1.24μH,
Rotor inertia in GD^2=0.024 kg-m^2

REFERENCES

[1] Guillermo Bossio, Cristian De Angelo, Guillermo Garcia, Jorge Solsona, Maria Ines Valla., "A 2D Model of the Induction Motor:, An Extension of the Modified Winding Function Approach", *Proceedings of 28th annual conference of the IEEE Industrial Electronics Society*, IECON2002, pp.62-67.

[2] Ghoggal A,.Aboubou A, .Zouzou S.E, Sahraoui M, Razik H, "Considerations about the modeling and simulation of airgap eccentricity in induction motors", *Proceedings of IEEE IECON Conference.*, Paris, France, 2006,pp.4987-4992.

[3] RajalakshmiSamaga and Dr.Vittal.K.P, "A Simplified Modeling Approach For Accounting Skewing Effect In Rotor Bars Of Squirrel Cage Induction Motor And Its Application In Motor Inductance Calculation", *Journal of Electrical Engineering*, Romania , Vol.10,December 2010

[4] Prof William T Thomson, "On-Line Motor Current Signature Analysis Prevents Premature Failure of large Induction Motor Drives", *Maintenance & asset management* | ME | ,Vol 24 no 3 May/June 2009.

[5] Randy Supangat, Jason Grieger,NeisimiErtugrul, Wen L. Soong, Douglas A. Gray and Colin Hansen, "Investigation Of Static Eccentricity Fault Frequencies Using Multiple Sensors In Induction Motors And Effects Of Loading",*IEEE Industrial Electronics,* IECON 2006, Nov2006 Page Nos:958-963

[6] Gojko Joksimovie M, MomirDurovic D, Penman J.,Neil Arthur, "Dynamic Simulation of Dynamic Eccentricity in Induction Machines- Winding Function Approach", *IEEE Transactions on Energy Conversion*, vol. 15,N02, June 2000,pp.143-148.

[7] Xiaodong Li, Qing Wu, Nandi S, "Performance analysis of a three phase induction machine with inclined static eccentricity", *IEEE Transactions on Industry Applications*, Vol.43,No2, March/April 2007,pp. 531-541.

[8] H.Hamidi, A.R. Nasiri and F.Taringoo, "Detection and Isolation of Mixed Eccentricity in Three Phase induction Motor Via Wavelet Packet decomposition", *5th Asian Control Conference*,2004, pp.1371-1375

[9] Jordi Cusido, Luis Romeral, Juan A. Ortega, Javier A. Rosero, Antonio Garcia Espinosa, "Fault detection in induction machines using power spectral density in wavelet decomposition" ,*IEEE Transactions on Industrial Electronics*, February 2008,vol. 55, no. 2, pp..633-643.

[10] Subhasis Nandi, Hamid A.Ttoliyat ,Xiaodong Li, "Condition Monitoring and Fault Diagnosis of Electrical Motors-A Review" ,I*EEE Transactions on Energy Conversion* ,VOL.20,NO.4,PP:719-729,December 2005.

[11] Jawad Faiz, Bashir Mahdi Ebrahim, Bilal Akin, Hamid A Toliyat, "Comprehensive Eccentricity Fault Diagnosis In Induction Motors Using Finite Element Method", IEEE Transactions on Magnetics, vol. 45, no. 3, March 2009, pp.1764-1767